

## Inclusive central region in perturbative Reggeon calculus\*

C. Pajares<sup>†</sup>

*High Energy Physics Division, Argonne National Laboratory, Argonne, Illinois 60439*

R. Pascual<sup>†</sup>

*Laboratoire de Physique Théorique et Particules Elementaires, Orsay, France*

(Received 19 January 1976)

The single-particle inclusive cross section and the correlation function are studied in the perturbative approach to Gribov's Reggeon calculus, evaluating the leading contributions to both functions. The large energy rise of the inclusive cross section appears as a consequence of the Pomeron having an intercept larger than 1. The same set of parameters which describes correctly the cross-section data and the triple-Regge region also describes the inclusive data in the central region.

### I. INTRODUCTION

In the last few years, Regge theory has been one of the theories most frequently used to explain the high-energy hadronic reactions. As is well known, the presence of Regge poles is accompanied by Regge cuts; a complete analysis of this as well as of the interactions among Reggeons was done in 1967 by Gribov and collaborators.<sup>1</sup> In those papers the Reggeon calculus was elaborated and it was shown that the small-angle behavior of hadronic amplitudes was equivalent to the infrared problem in a field theory in  $1+2$  dimensions. Further progress in this direction has been done using renormalization-group and  $\epsilon$ -expansion techniques, a review of which can be found in Ref. 2. Nevertheless, the results obtained will describe the amplitude behavior at energies much higher<sup>3</sup> than those available with the present accelerators so that in order to explain the present experimental data another approach must be used.

Phenomenology of Gribov's calculus has been done<sup>4</sup> in the case of the so-called weak-coupling version, in which the coupling of three Pomerons vanishes at  $t=0$ . In this approach, the leading terms to the total cross section, differential cross section, and distribution momenta<sup>5,6</sup> have been evaluated as well as classified in terms of the two-component model.<sup>7</sup> The weak-coupling version is able to explain the behavior and structure of the total and differential cross section at CERN ISR and Fermilab energies, although it does not fit the data in the central region of the single-particle inclusive cross section<sup>8</sup> if one uses the values of the parameters which fit the cross-section data, and it also has difficulties in describing the cross-section behavior in the PS energy region. Another failure of this version is the non-existence of the predicted dip at small angles in

the triple-Regge region<sup>9</sup>; independent of the arguments which attribute the nonexistence of the dip to terms other than the *PPP* (see Ref. 10) (for instance, absorptive corrections<sup>11</sup>), it seems that all these facts indicate the nonvalidity of the weak-coupling version.

On the other hand, fits to total and differential cross sections at all energies have shown that the data seem to choose a leading Pomeron whose intercept is higher than 1.<sup>12</sup> This fact has been incorporated in a perturbative approach to the Gribov Reggeon calculus<sup>13</sup>; if we call  $r$  the triple-Pomeron coupling at  $t=0$  and  $\alpha'$  the slope of the bare Pomeron, the expansion is done in powers of  $(r^2/8\pi\alpha') \ln s$ , which, if  $r$  is taken of the same order as the value obtained from the inclusive spectrum ( $r \approx 1 \text{ GeV}^{-2} \text{ mb}^{-1/2}$ ), is of the order of  $10^{-2} \ln s$ , which is really a small number at available energies. Considering the main diagrams in such an expansion, one finds good agreement with the experimental data on cross sections if one takes  $\alpha(0)$  slightly larger than 1 [ $\alpha(0) \approx 1.12$ ]. (Notice<sup>14</sup> that such a solution is not in contradiction with the Froissart bound nor with  $t$ -channel unitarity.)

In this paper we will use this perturbative approach to study, in the central region, the one-particle inclusive cross sections as well as the correlations in the double-particle inclusive spectrum. In Sec. II we calculate the contribution of the leading diagrams to the single-particle spectrum in the central region using the cutting rules of Abramovskii, Gribov, and Kancheli (AGK)<sup>5</sup>; our results differ from those in Refs. 5 and 6 due to the fact that our *PPP* coupling is not zero at  $t=0$ . In Sec. III we study the diagrams which contribute to the correlation function. In Sec. IV our results are compared with the experimental data, emphasizing the compatibility of our value for the parameters with those ob-

tained from the small-angle data. Finally, the conclusions are presented in Sec. V.

## II. SINGLE-PARTICLE INCLUSIVE SPECTRUM

Let us consider the reaction  $a + b \rightarrow c + X$  when  $c$  is in the central region. Figure 1 shows the diagrams which give the main contribution to the inclusive cross section. Let us define

$$\begin{aligned}\xi &= \ln s = \ln(p_a + p_b)^2, \\ \eta_1 &= \ln s_1 = \ln(p_a - p_c)^2, \\ \eta_2 &= \ln s_2 = \ln(p_b - p_c)^2,\end{aligned}\quad (1)$$

which are related through

$$\xi = (\eta_1 + \eta_2) - \ln K \simeq \eta_1 + \eta_2, \quad (2)$$

where we have used the fact that the transverse mass  $K \equiv m_c^2 + p_{\perp c}^2 = s_1 s_2 / s$  is negligible in front of  $\eta_1 + \eta_2$  in the central region. In terms of  $\eta_1$  and  $\eta_2$ , the rapidity of particle  $c$  in the center of mass,  $y$ , is given by

$$y = \frac{1}{2}(\eta_1 - \eta_2). \quad (3)$$

We will denote by  $g_i(q^2)$  the coupling of the Pomeron to particle  $i$  and by  $r$  the triple-Pomeron vertex, which will be parametrized<sup>13</sup> as

$$\begin{aligned}g_i(q^2) &= g_i \exp(-A_i q^2/2), \\ r(q_1^2, q_2^2, q_3^2) &= r \exp[-B(q_1^2 + q_2^2 + q_3^2)/2].\end{aligned}\quad (4)$$

$$y_1 = -\frac{\lambda g_a g_b \gamma_0}{16\pi} \int_0^\infty dk^2 g_a^2(k^2) r(0, k^2, k^2) \int_\Lambda^{\eta_1} d\xi_1 e^{\Delta \xi_1} e^{[2\alpha(k^2)-2](\eta_1 - \xi_1)} e^{\Delta \eta_2}, \quad (7)$$

where  $\lambda \simeq 1.12$  is an enhancement factor introduced in order to take into account (via duality arguments) the possible intermediate states in the top of the diagrams, and  $\Lambda \simeq \ln 5$  is a cutoff.<sup>13</sup> Introducing in (7) the parametrization (4) one gets by integration (Ei is the exponential-integral function)

$$y_1 = \frac{-\lambda g_a^2 g_b r \gamma_0}{16\pi 2\alpha'} e^{\Delta \xi} \exp\left[-(A_a + B) \frac{\Delta}{2\alpha'}\right] \left[ \text{Ei}\left(\Delta \left(\frac{A_a + B}{2\alpha'} + \eta_1 - \Lambda\right)\right) - \text{Ei}\left(\Delta \frac{A_a + B}{2\alpha'}\right) \right], \quad (8)$$

$$y_2 = \frac{-\lambda g_b^2 g_a r \gamma_0}{16\pi 2\alpha'} e^{\Delta \xi} \exp\left[-(A_b + B) \frac{\Delta}{2\alpha'}\right] \left[ \text{Ei}\left(\Delta \left(\frac{A_b + B}{2\alpha'} + \eta_2 - \Lambda\right)\right) - \text{Ei}\left(\Delta \frac{A_b + B}{2\alpha'}\right) \right]. \quad (9)$$

The contribution of the diagrams of Figs. 1(d) and Fig. 1(e), denoted by  $L_1$  and  $L_2$ , can be calculated in an analogous way; we have

$$L_1 = -\frac{g_a g_b \gamma_0}{16\pi} \int_0^\infty dk^2 r^2(0, k^2, k^2) \int_\Lambda^{\eta_1 - \Lambda} d\xi_1 \int_\Lambda^{\eta_1 - \xi_2} d\xi_2 e^{\Delta(\xi_1 + \xi_2)} e^{[2\alpha(k^2)-2](\eta_1 - \xi_1 - \xi_2)} e^{\Delta \eta_2}, \quad (10)$$

which after integration becomes

$$\begin{aligned}L_1 = & -\frac{g_a g_b r^2 \gamma_0}{16\pi 2\alpha'} \exp[\Delta(\xi - B/\alpha')] \left\{ \left(\frac{B}{\alpha'} + \eta_1 - 2\Lambda\right) \left[ \text{Ei}\left(\Delta \left(\frac{B}{\alpha'} + \eta_1 - 2\Lambda\right)\right) - \text{Ei}\left(\Delta \frac{B}{\alpha'}\right) \right] \right. \\ & \left. + \frac{1}{\Delta} \exp\left(\frac{\Delta B}{\alpha'}\right) \{1 - \exp[(\eta_1 - 2\Lambda)\Delta]\} \right\}\end{aligned}\quad (11)$$

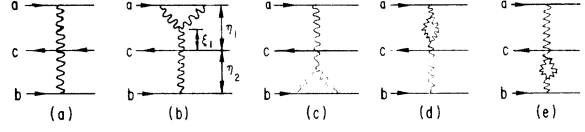


FIG. 1. Leading contributions to the single-particle inclusive spectrum.

We will represent by  $\psi(q_\perp^2)$  the two-particle-two-Pomeron vertex, which will be parametrized by

$$\psi(q_\perp^2) \equiv \int d^2 p_{c\perp} \psi(p_{c\perp}^2, q_\perp^2) = \gamma_0 e^{-\eta_1 q_\perp^2}, \quad (5)$$

where  $q_\perp$  is the momentum carried by the Pomeron. (The assumption that  $\psi$  does not depend on  $p_{c\perp} \cdot q_\perp$  implies that there are no long-range azimuthal correlations.) We will also use  $\Delta \equiv \alpha(0) - 1$ .

With this notation, the contribution of the diagram of Fig. 1(a) to the inclusive cross section will be

$$P = g_a g_b e^{\Delta \xi} \gamma_0. \quad (6)$$

The contributions of the diagrams of Figs. 1(b) and 1(c) (denoted  $y_1$  and  $y_2$ ) are calculated in the same way as in Ref. 13; for example,

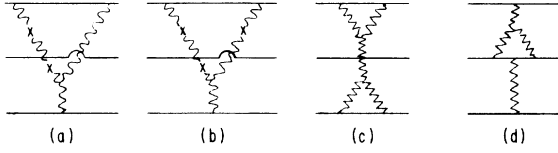


FIG. 2. (a) and (b) Typical cancellations in the single-particle inclusive spectrum. (c) and (d) Diagrams neglected in formula (12).

and the equivalent expression for  $L_2$  obtained from (11) by changing  $\eta_1 \leftrightarrow \eta_2$ .

Therefore, the single-particle inclusive cross section is given by

$$\frac{d\sigma}{dy} = P + y_1 + y_2 + L_1 + L_2. \quad (12)$$

In this expression we have not taken into account the contribution of other diagrams such as those shown in Fig. 2. It is easy to see that the diagrams corresponding to Figs. 2(a) and Fig. (2b) cancel each other as a consequence of the AGK cutting rules. The diagram in Fig. 2(c) is of second order in  $r$  and therefore of the same order as  $L_1$  and  $L_2$ . However, numerical computation shows that its contribution is much smaller than that of the diagrams in Fig. 1. Finally the diagram shown in Fig. 2(d) has been neglected; such a diagram contains the two-particle-three-Pomeron coupling and will be zero if  $\alpha(0) = 1$ .<sup>15</sup> In our case the argument cannot be applied, and the diagram can be calculated if we use some model for the coupling. However, if we include it in (12) we will need to fix the parameter  $\gamma_0$ ; otherwise, it would not be necessary to fix it since we are not worried about the absolute normalization of the inclusive cross section. Since we expect that its contribution will be small, we will neglect it for simplicity.

### III. CORRELATIONS

Let us consider the double-particle inclusive reaction  $a + b \rightarrow c + d + X$  when the particles  $c$  and  $d$  are produced in the central region. As before, we define

$$y_1^c = \frac{4g^3 r \gamma_0^2 \lambda}{16\pi 2\alpha'} \exp \left[ \Delta \left( \xi - \frac{A_b + B + 2\gamma_1}{2\alpha'} \right) \right] \left[ \text{Ei} \left( \Delta \left( \frac{A_b + B + 2\gamma_1}{2\alpha'} + \xi - \eta_1 \right) \right) - \text{Ei} \left( \Delta \left( \frac{A_b + B + 2\gamma_1}{2\alpha'} + \xi - \Lambda \right) \right) \right]. \quad (19)$$

The expression for  $y_2^c$  is identical to (19) changing  $A_b \rightarrow A_a$  and  $\eta_1 \rightarrow \eta_3$ .

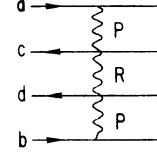


FIG. 3. PRP diagram contribution to the correlation function.

$$\begin{aligned} \eta_1 &= \ln(p_a - p_c)^2, \\ \eta_2 &= \ln(p_c + p_d)^2, \\ \eta_3 &= \ln(p_b - p_d)^2, \end{aligned} \quad (13)$$

and we have, neglecting the transverse masses,

$$\xi = \ln(p_a + p_b)^2 \simeq \eta_1 + \eta_2 + \eta_3. \quad (14)$$

In terms of  $\eta_i$  the center-of-mass rapidities will be

$$\begin{aligned} y_c &= \frac{1}{2}(\eta_2 + \eta_3 - \eta_1), \\ y_d &= \frac{1}{2}(\eta_3 - \eta_1 - \eta_2). \end{aligned} \quad (15)$$

We are interested in calculating the correlation function

$$C(y_c, y_d) = \frac{1}{\sigma} \frac{d\sigma}{dy_c dy_d} - \frac{1}{\sigma^2} \frac{d\sigma}{dy_c} \frac{d\sigma}{dy_d}. \quad (16)$$

The main contribution to  $C$  comes from the diagram of Fig. 3, where  $R$  is a Reggeon of  $\alpha_R(0) \simeq \frac{1}{2}$  and is given by

$$C(y_c, y_d) \sim \exp\left(-\frac{1}{\lambda} |y_c - y_d|\right), \quad \lambda \simeq 2. \quad (17)$$

The other diagrams which give a nonzero contribution are those shown in Fig. 4, and are the ones in which we are interested.

The diagram in Fig. 4(a) gives a contribution

$$\begin{aligned} C_1 &= \lambda^2 \int \frac{d^2 K}{(2\pi)^2} g^4(K^2) \exp[(2\alpha(K^2) - 2)\xi] \gamma^2(K^2) \\ &= \frac{\lambda^2 g^4 \gamma_0^2}{2(2\pi)} \frac{\exp(2\Delta\xi)}{2A + 2\gamma_1 + 2\alpha'\xi}. \end{aligned} \quad (18)$$

The diagrams of Figs. 4(b) and 4(c) give a contribution  $y_1^c$  and  $y_2^c$ , and those of Figs. 4(d) and 4(e) will be denoted by  $L_1^c$  and  $L_2^c$ ; the computation is straightforward and the result is

$$\begin{aligned}
L_1^c = & -\frac{4g^2r^2\gamma_0^2}{16\pi 2\alpha'} \exp\left[\Delta\left(\xi - \frac{B+\gamma_1}{\alpha'}\right)\right] \\
& \times \left[ \left(\frac{B+\gamma_1}{\alpha'} + \eta_1 + \eta_2 - \Lambda\right) \text{Ei}\left(\Delta\left(\frac{B+\gamma_1}{\alpha'} + \eta_1 + \eta_2 - \Lambda\right)\right) - \left(\frac{B+\gamma_1}{\alpha'} + \eta_2\right) \text{Ei}\left(\Delta\left(\frac{B+\gamma_1}{\alpha'} + \eta_2\right)\right) \right. \\
& + \left(\frac{B+\gamma_1}{\alpha'} + \eta_2 + \eta_3 - \Lambda\right) \text{Ei}\left(\Delta\left(\frac{B+\gamma_1}{\alpha'} + \eta_2 + \eta_3 - \Lambda\right)\right) - \left(\frac{B+\gamma_1}{\alpha'} + \xi - 2\Lambda\right) \text{Ei}\left(\Delta\left(\frac{B+\gamma_1}{\alpha'} + \xi - 2\Lambda\right)\right) \\
& \left. + \frac{1}{\Delta} \exp\left(\Delta\frac{B+\gamma_1}{\alpha'}\right) \left\{ \exp(\Delta\eta_2) - \exp[\Delta(\eta_1 + \eta_2 - \Lambda)] + \exp[\Delta(\xi - 2\Lambda)] - \exp[\Delta(\eta_2 + \eta_3 - \Lambda)] \right\} \right], \quad (20)
\end{aligned}$$

$$\begin{aligned}
L_2^c = & \frac{g^2r^2\gamma_0^2}{16\pi 2\alpha'} \exp\left[\Delta\left(\xi - \frac{B}{\alpha'}\right)\right] \left\{ \frac{1}{\Delta} \exp(B\Delta/\alpha') \left[ 1 - \exp[\Delta(\xi - \eta_1 - \eta_3)] \right] \right. \\
& \left. + \left(\frac{B}{\alpha'} + \xi - \eta_1 - \eta_3\right) \left[ \text{Ei}\left(\Delta\left(\frac{B}{\alpha'} + \xi - \eta_1 - \eta_3\right)\right) - \text{Ei}\left(\Delta\frac{B}{\alpha'}\right) \right] \right\}. \quad (21)
\end{aligned}$$

Collecting terms, the correlation function will be given by expression (17) plus the five terms

$$(C_1 + y_1^c + y_2^c + L_1^c + L_2^c)/\sigma, \quad (22)$$

where terms which cancel out if  $\sigma$  in Eq. (16) is  $g^2$  have been neglected. Notice that, as in Ref. 6, we obtain three terms more than in Ref. 5:  $C_1$ ,  $y_1^c$ , and  $y_2^c$ . On the other hand, we do not have the relation  $L_2^c = -\frac{1}{4}L_1^c$  obtained in Ref. 5 owing to the dependence on the loop momenta of the coupling  $\psi$  which makes  $L_2^c$  and  $L_1^c$  no longer related by a simple factor.

#### IV. COMPARISON WITH THE EXPERIMENTAL DATA

##### A. Single-particle inclusive spectrum

The most significant aspect of the single-particle inclusive spectrum in the central region is the existence of a rapidity plateau. Experimentally it is not completely flat, but its slope is not larger than 10%; furthermore, its value increases with the energy. The increase depends on which particle is detected; it is very large for  $K^-$  and  $\bar{p}$  in  $pp$  collisions because of threshold effects,<sup>16</sup> but for other particles it is not so large. Until recently the data showed an increase of about 10% when  $\ln s$  changes from 6 to 8, but more recent data<sup>17</sup> indicate an increase of about 40%. This increase

cannot be explained as a consequence of secondary trajectories.<sup>18</sup> We will not consider these secondary trajectories but will try to see if the effect of diagrams 1(b)–1(e) is able to explain the experimental increase without destroying the plateau. In order to do that we introduce in formula (12) the same parameters which explain the two-body cross sections,<sup>13</sup> studying which are the ranges of  $r$  and  $\Delta$  which do not destroy the plateau in more than 10% and give an increase of 40% when  $\xi$  varies from 6.2 to 8.2. The parameter  $\gamma_0$  which appears in all terms of formula (12) is not taken into account because we are not worried about the absolute normalization. (For a given set of parameters, it can always be fixed from the multiplicity data.)

Numerical computation of formula (12), in which particles  $a$  and  $b$  are protons, shows that unless one uses values of  $C = rg^3/16\pi$  larger than 6 and values of  $\Delta$  larger than 0.14 the plateau will always be present with a very small curvature. This fact was expected from formula (12). In this formula the dependence on  $y$  comes from the arguments of the Ei functions; expanding these functions and collecting the terms which arise from  $y_1$  and  $y_2$  and those coming from  $L_1$  and  $L_2$ , one realizes the weak dependence on  $y$ . For example, in the combination  $y_1 + y_2$  appear the terms

$$\begin{aligned}
& \text{Ei}\left(\Delta\left(\frac{A+B}{2\alpha'} + \eta_1 - \Lambda\right)\right) + \text{Ei}\left(\Delta\left(\frac{A+B}{2\alpha'} + \eta_2 - \Lambda\right)\right) \\
& = 2G + \Delta\left(\frac{A+B}{\alpha'} + \xi - 2\Lambda\right) + \frac{\Delta^2}{2}\left(\frac{A+B}{2\alpha'}\right)^2 + \frac{\Delta^2}{2}\frac{A+B}{2\alpha'}(\xi - 2\Lambda) \\
& + \frac{\Delta^2}{4}\left(\frac{(\xi - 2\Lambda)^2}{2} + 2y^2\right) + \ln\left|\Delta^2\left(\frac{A+B}{2\alpha'}\right)^2 + \Delta^2\frac{A+B}{2\alpha'}(\xi - 2\Lambda) + \Delta^2\left(\frac{(\xi - 2\Lambda)^2}{4} + y^2\right)\right| + O(\Delta^3),
\end{aligned}$$

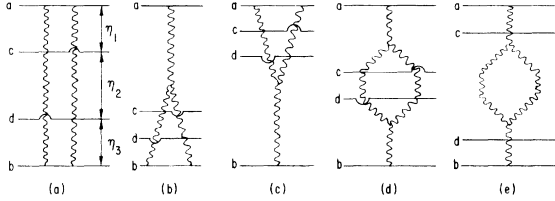


FIG. 4. Leading contributions to the correlation function.

which really have weak  $y$  dependence unless  $\Delta$  becomes large.

Numerically the increase of the plateau with the energy depends on  $C$  and  $\Delta$  in such a way that fixed  $C$  [as a consequence of the factor  $\exp(\Delta\xi)$ ] increases with  $\Delta$ , but such an increase decreases when  $C$  increases. For  $C=1$  (the value preferred for data on the triple-Regge region), the increase is of 10% for  $\Delta=0.06$  and of 30% for  $\Delta=0.14$ . For  $C=2$  the respective values are 10% and 25%. Notice that although the increase obtained is mainly due to using a Pomeron with intercept larger than 1, in the same way in which such a Pomeron causes an increase of the total cross section, the quantitative increasing of the total cross section and the inclusive cross sections is different because there is no one-to-one correspondence between the leading diagrams contributing to both quantities. It could be thought that, since the ISR energies, where we study the inclusive behavior, correspond to energies where the total cross sections are almost flat [ $s \approx (3000)^{1/2}(m_\pi^2 + \langle p_\perp^2 \rangle) \approx 20 \text{ GeV}^2$ ], to the increasing of the inclusive cross section will correspond an increasing of the total cross section in the range where the data are flat. In fact, this increase of the Pomeron diagrams exists but is compensated with the decreasing contributions of ordinary trajectories.<sup>13</sup> (To accomplish this, it is necessary to break the exchange degeneracy, which is done naturally in the model owing to the existence of triangular diagrams  $\pi\pi f$  which do not appear in the  $\omega$  contribution.<sup>13</sup>) The inclusion of ordinary trajectories in the inclusive spectrum is more complicated than in the total cross section owing to the vertex  $\gamma_{PR}^c$ ,<sup>18</sup> however, all the studies<sup>18</sup> using Pomerons of intercept 1 do not predict any large energy dependence of the  $PR$  terms at ISR energies, which induces one to think that the energy increase predicted by the Pomeron diagrams is not disturbed by ordinary Reggeons.

### B. Correlations

When particles  $c$  and  $d$  are in the central region, their correlation function is compatible within the experimental errors with the exponential form

(17). We want to see if, for the previous values of the parameters, the diagrams of Fig. 4 do not destroy either the exponential form (17) or its energy independence. In other words, the diagrams of Fig. 4 must be almost independent of the rapidities and of the energy.

In formula (22) we have, besides the irrelevant  $\gamma_0$  parameter which is obtained by normalization, the slope  $\gamma_1$ , which is difficult to evaluate. In Ref. 6 it has been calculated in a model-dependent way, and the authors suggest  $\gamma_1 \approx 10 \text{ GeV}^{-2}$ ; however, large variations from this value are permissible. We will leave  $\gamma_1$  as a free parameter.

Numerically, it is found that for any reasonable value of  $\Delta$  ( $0.06 < \Delta < 0.13$ ) and  $C$  ( $0.5 < C < 4$ ), the contribution of the diagrams of Fig. 4 to the correlation function in the central region is independent of the rapidities  $y_c$  and  $y_d$ . (The changes of the rapidities never change the correlation function by more than 10%.) This means that the exponential form (17) will not be destroyed.

The contribution to  $c(y_c, y_d)$  comes mainly from diagram 4(a); next in importance is 4(d) for large  $\gamma_1$  values. For  $\gamma_1=0$  the contribution of 4(d) is negligible but for  $\gamma_1=10 \text{ GeV}^{-2}$  it is larger than that of 4(a). Diagrams 4(b), 4(c), and 4(e) never give a contribution larger than 10% of that of 4(a).

Finally we have studied the energy dependence of  $c(0,0)$ . We have found that  $c(0,0)$  increase with energy depending on the value of  $\gamma_1$  and  $\Delta$ . The larger the value of  $\Delta$  the larger the increase, which is quite insensitive to the value of  $C$ . The increase is also larger for large values of  $\gamma_1$ . For the values  $C=1$ ,  $\Delta=0.12$  we find that the increase is (for  $\xi=6$  to  $\xi=8$ ) of 32%, 38%, and 42% for  $\gamma_1=0$ , 5, and  $10 \text{ GeV}^{-2}$ , respectively.

### V. CONCLUSIONS

We have computed the leading contributions to the single-particle inclusive spectrum and to the correlation function in the perturbative approach of the Gribov Reggeon calculus, with a bare Pomeron whose intercept is larger than 1, showing that there exists a set of values of the triple-Pomeron coupling  $\gamma$  and  $\Delta$ , which, besides describing the cross-section data and the triple-Regge region, is also able to explain the behavior of the single-particle inclusive spectrum in the central region as well as the main features of the correlation function. According to this picture, the recently reported large increase with energy of the single-particle inclusive spectrum is just another manifestation of a bare Pomeron whose intercept is larger than 1. [The momentum-distribution data also support a bare Pomeron with intercept larger than 1.<sup>20</sup>] A similar increase with the energy of

the correlation function is predicted.

Our results are obtained in the perturbative expansion framework with the additional ingredient of the AGK cutting rules. As far as these rules seem to work,<sup>19</sup> our results only depend on the basic assumptions of the perturbative approach. It is thought that minor approximations done in this work [such as neglecting diagram 2(d)] do not basically change our results.

#### ACKNOWLEDGMENTS

We are grateful to A. Capella and J. Kaplan for useful discussions. We thank the High Energy Physics Division of Argonne and the LPTPE of Orsay for their kind hospitality, also, the G.I.F.T. for financial support.

\*Work performed under the auspices of the United States Energy Research and Development Administration.

†Visitor from the Universidad Autónoma de Barcelona, Bellaterra, Barcelona, Spain.

- <sup>1</sup>V. N. Gribov, Zh. Eksp. Teor. Fiz. 53, 654 (1967) [Sov. Phys.—JETP 26, 414 (1968)]; V. N. Gribov and A. A. Migdal, *ibid.* 55, 1498 (1968) [*ibid.* 28, 784 (1969)]; Yad. Fiz. 8, 1002 (1968) [Sov. J. Nucl. Phys. 8, 558 (1969)]; *ibid.* 8, 1213 (1968) [8, 703 (1969)].
- <sup>2</sup>H. D. I. Abarbanel, J. B. Bronzan, R. Sugar, and A. R. White, Phys. Rep. 21C, 119 (1975).
- <sup>3</sup>D. Amati and R. Jengo, Phys. Lett. 56B, 465 (1975).
- <sup>4</sup>C. Pajares D. Schiff, Lett. Nuovo Cimento 8, 237 (1973); J. N. Ng and U. P. Sukhatme, Nucl. Phys. B55, 253 (1973); B70, 229 (1974); N. S. Craigie and G. Preparata, Phys. Lett. 45B, 487 (1973).
- <sup>5</sup>V. A. Abramovskii, V. N. Gribov, and O. V. Kancheli, Yad. Fiz. 18, 595 (1973) [Sov. J. Nucl. Phys. 18, 308 (1974)].
- <sup>6</sup>M. Creutz, F. E. Paige, and Pu Shen, Phys. Rev. D 9, 684 (1974).
- <sup>7</sup>K. A. Ter-Martirosyan, Phys. Lett. 44B, 179 (1973); U. P. Sukhatme and C. Pajares, Phys. Rev. D 9, 2119 (1974).
- <sup>8</sup>C. Pajares (unpublished).
- <sup>9</sup>Dubna-Fermilab-Rockefeller-Rochester Collaboration, A. S. Carroll *et al.*, report presented at the XVII International Conference on High Energy Physics, London, 1974 (unpublished).
- <sup>10</sup>J. Gabarro and C. Pajares, Nucl. Phys. B64, 493 (1973).
- <sup>11</sup>J. L. Cardy, Nucl. Phys. B56, 605 (1973).
- <sup>12</sup>P. D. B. Collins, F. D. Gault, and A. Martin, Phys. Lett. 47B, 171 (1973); Nucl. Phys. B80, 135 (1974).
- <sup>13</sup>A. Capella and J. Kaplan, Phys. Lett. 52B, 448 (1974); A. Capella, J. Kaplan, and J. Tran Thanh Van, Nucl. Phys. B97, 493 (1975).
- <sup>14</sup>J. B. Bronzan and R. L. Sugar, Phys. Rev. D 8, 3049 (1973); J. L. Cardy, Nucl. Phys. B75, 413 (1974).
- <sup>15</sup>C. E. Jones, F. E. Low, S. H. Tye, G. Veneziano, and J. E. Young, Phys. Rev. D 6, 1033 (1972).
- <sup>16</sup>R. Jengo, A. Krzywicki, and B. Petersson, Phys. Lett. 43B, 397 (1973); E. J. Squires and D. M. Webber, Lett. Nuovo Cimento 7, 193 (1973); Chan Hong-Mo, H. I. Miettinen, D. P. Roy, and P. Hoyer, Phys. Lett. 40B, 406 (1972); L. Caneschi, Nucl. Phys. B68, 77 (1974).
- <sup>17</sup>British-Scandinavian collaboration, B. Alper *et al.*, Nucl. Phys. B100, 237 (1975).
- <sup>18</sup>J. R. Freeman and C. Quigg, Phys. Lett. 47B, 39 (1973); R. C. Brower, R. N. Cahn, and J. Ellis, Phys. Rev. D 7, 2080 (1973); T. Inami, Nucl. Phys. B77, 337 (1974).
- <sup>19</sup>O. K. Kaucheli, Zh. Eksp. Teor. Fiz. Pis'ma Red. 18, 465 (1975) [JETP Lett. 18, 274 (1973)]; E. S. Lehman and G. A. Winbow, Phys. Rev. D 10, 2962 (1974); C. Pajares, in Proceedings of the Third Winter Meeting on Fundamental Physics, Sierra, Nevada, 1975 (unpublished); L. Caneschi and A. Schwimmer, Nucl. Phys. B102, 381 (1976).
- <sup>20</sup>D. R. Snider and H. W. Wyld, Phys. Rev. D 11, 2538 (1975).